Available online at www.sciencedirect.com
ScienceDirect
Bioelectrochemistry 70 (2007) 501 – 507
Bioelectrochemistry
www.elsevier.com/locate/bioelechem

Real time electroporation control for accurate and safe in vivo non-viral gene therapy

David Cukjati [a,b], Danute Batiuskaite [a,c], Franck André [a], Damijan Miklavčič [b], Lluis M. Mir [a,*]

[a] UMR 8121 CNRS, Institute Gustave–Roussy, 39 Rue Camille Desmoulins, F-94805 Villejuif Cédex, France
[b] University of Ljubljana, Faculty of Electrical Engineering, Laboratory of Biocybernetics, Tržaška 25, SI-1000 Ljubljana, Slovenia
[c] Vytautas Magnus University, Faculty of Natural Sciences, Department of Biology, Vileikos 8, LT-44404 Kaunas, Lithuania

Received 21 August 2006; received in revised form 5 November 2006; accepted 6 November 2006
Available online 10 November 2006

Abstract

In vivo cell electroporation is the basis of DNA electrotransfer, an efficient method for non-viral gene therapy using naked DNA. The electric pulses have two roles, to permeabilize the target cell plasma membrane and to transport the DNA towards or across the permeabilized membrane by electrophoresis. For efficient electrotransfer, reversible undamaging target cell permeabilization is mandatory. We report the possibility to monitor in vivo cell electroporation during pulse delivery, and to adjust the electric field strength on real time, within a few microseconds after the beginning of the pulse, to ensure efficacy and safety of the procedure. A control algorithm was elaborated, implemented in a prototype device and tested in luciferase gene electrotransfer to mice muscles. Controlled pulses resulted in protection of the tissue and high levels of luciferase in gene transfer experiments where uncorrected excessive applied voltages lead to intense muscle damage and consecutive loss of luciferase gene expression.

Keywords: DNA electrotransfer; Gene therapy; Electropermeabilization; Electroporation; Electrochemotherapy; Finite element modeling

1. Introduction

Biotechnological and biomedical applications of in vivo delivery of short high voltage pulses, like in vivo DNA electrotransfer, also termed electrogenetherapy, are rapidly developing [1–5]. For efficient in vivo gene transfer, it is necessary to inject DNA into the tissue and to achieve cell plasma membrane permeabilization [6]. Increased membrane permeability results from supraphysiological transmembrane voltages induced by external electric pulses [7–9]. Mechanisms of DNA electrotransfer in vivo have recently been described [6,10]. The two key steps are the permeabilization of the target cells plasma membrane by electroporation and the electrophoresis of the DNA within the tissue. These two effects can be obtained separately using the appropriate sequence of electric pulses: short (100 μs) square-wave high voltage pulses (HV) that permeabilize the cells without substantial DNA transport to the cells and long (100 ms) low voltage pulses (LV), that are instrumental in facilitating the DNA transfer into the cells [6]. Even though gene transfer efficacy, measured by gene expression level, depends on the characteristics of the electrophoretic long low voltage pulse, target cell permeabilization is mandatory for efficient gene transfer. Moreover, for a safe gene transfer, electropermeabilization, also termed electroporation, must be reversible, that is not excessive, in order to avoid permanent cell damage. Optimal parameters for in vivo electroporation can be determined using in vivo tests for cell permeabilization [11] after the pulse, like the one based on 51Cr-EDTA uptake [12], and by using mathematical modeling to determine electric field distribution [13,14]. However, it would be much better to control cell permeabilization during the pulse delivery in order to ascertain that (reversible) cell permeabilization will be actually achieved at the end of the pulse, as well as to prevent excessive (irreversible) permeabilization [11,13,15]. Real time control of electroporation appears thus critical for this non-viral gene transfection method that has many advantages with respect to viral methods.

Here, we report that in vivo electroporation can be precisely computer-controlled to ascertain that permeabilization will be achieved at the end of the pulse, while at the same time permanent cell damage is prevented. We demonstrate that the temporal progression of tissue electroporation can be detected in real time

* Corresponding author. Tel.: +33 1 42114792; fax: +33 1 42115276.
E-mail address: luismir@igr.fr (L.M. Mir).

1567-5394/$ - see front matter © 2006 Elsevier B.V. All rights reserved.
doi:10.1016/j.bioelechem.2006.11.001

at the beginning of the pulse on the basis of current and voltage measurements made during pulse delivery to tissues. Then, adjustment of the pulse voltage in real time ensures cell membrane *reversible* permeabilization, which is necessary for efficient in vivo DNA electrotransfer. Using optimized LV parameters, real time control of HV, as reported here, results then in safe and efficient gene transfer.

2. Materials and methods

Female Wistar rats (Janvier) were handled according to recommended good practices [16] and institutional ethics rules for animal experimentation. They were anesthetized by means of the intraperitoneal administration of Ketamine (100 mg/kg; Panpharma) and Xylazine (10 mg/kg; Bayer). Pulses were directly delivered to rat skeletal muscle and liver through two plate electrodes placed as shown in Fig. 1a. Plate electrodes consisted of two parallel metal plates, separated by 5.7 mm for skeletal muscles and by 4.4 mm for liver. One experiment per rat extremity (*triceps brachii* muscle of the hind limb and *gastrocnemius medialis* muscle of the forelimb) was performed. Liver tissue was accessed by midventral incision in the abdominal wall which was sewed up after pulses application. To parallel the liver treatment, electrodes were applied directly on the skeletal muscles after incision of the skin in the back part of the limb. Four separate sites were exposed to the electric pulses in each rat liver. Good contact between the electrodes and tissue was assured by a conductive gel (EKO-GEL, Egna).

In experiments reported in Figs. 2 and 3, 8 square-wave pulses of 100 μs duration were delivered at a repetition frequency of 1 Hz by a PS 15 electropulsator (Jouan). Rise time of the pulses was 0.6 to 2.1 μs while fall time was 2 μs. High voltage probe PK 2 kV (LeCroy), coil wide band current transformer model 5124 (Pearson Electronics) and digital oscilloscope (Waverunner, LeCroy) were used to measure store voltage and current for 200 μs after the beginning of each of the eight pulses with sampling rate between 25 and 100 MSamples/s (Fig. 2a). Each current sample was divided by the corresponding voltage sample to yield conductance ($g = I/U$). Conductance was defined only when voltage was nonzero (Fig. 2b). For muscle, amplitude of the voltage pulses was varied from 50 to 320 V and for liver from 50 to 550 V.

The electric field strength in the tissue was estimated using a finite element numerical model of the electric field distribution in muscle and liver (Fig. 1b) that we have previously validated in experiments in rabbit liver [13]. Electric field strength calculations were made with a commercial program (EMAS, Ansoft, USA) [17].

200 μl of ^{51}Cr-EDTA (Amersham) with a specific activity of 3.7 MBq/ml were injected intravenously, 5 or 4 min before the electric pulses delivery to muscle or liver respectively. The injected ^{51}Cr-EDTA distributes freely in the vascular and extracellular compartments, but does not enter the intracellular compartments unless access is provided, e.g. by electroporation. Animals were sacrificed 24 h after ^{51}Cr-EDTA injection. Tissues exposed to electric pulses were taken out, weighed and counted in a Cobra 5002 gammacounter (Packard Instruments). The net ^{51}Cr-EDTA uptake as a result of electropermeabilization was calculated as the measured activity (converted to nanomoles of ^{51}Cr-EDTA) per gram of the tissue exposed to the electric pulses. ^{51}Cr-EDTA uptakes were used to calculate mean values of uptake (± SEM) as a function of the ratio of the applied voltage to electrodes distance, in the rat skeletal muscle and in liver. Solid (muscle), dashed (liver) and dotted (muscle, transcutaneous pulses) lines in Fig. 3a present linear regressions to field intensities corresponding to low uptake values, increasing uptake values, and decreasing uptake values. Electric field strength threshold values of reversible and irreversible

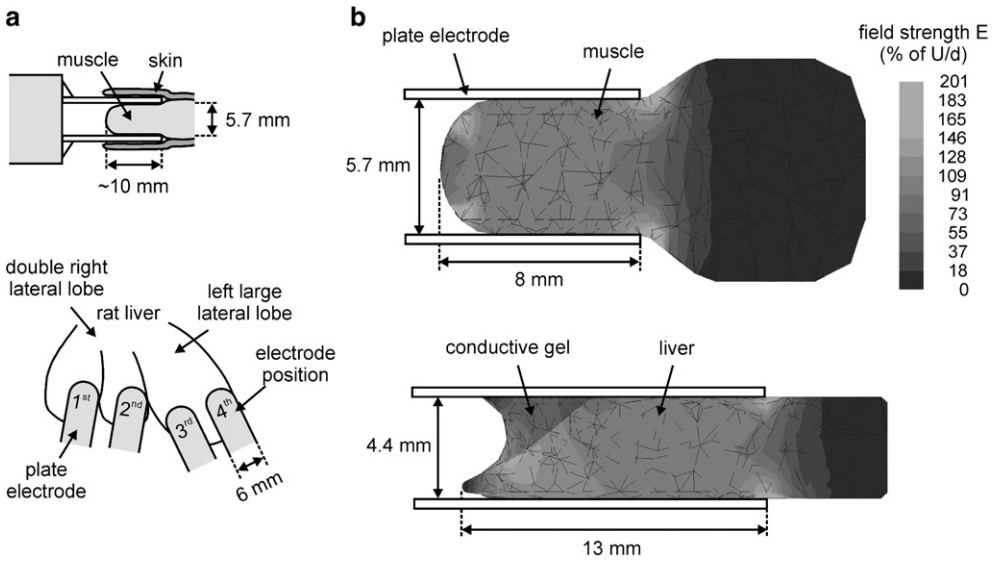

Fig. 1. Electrode positioning and electric field strength distribution. (a) Electrode positioning in rat skeletal muscle and liver (left lobe appears on the right side as animals are lying on the back for the surgical access to the liver). (b) Estimated electric field strength distributions calculated by the finite elements method are presented in cross sections of muscle and liver tissues between the two plate electrodes. Electric field strength (E) is reported as percent of the applied voltage (U) to electrode distance (d) ratio.

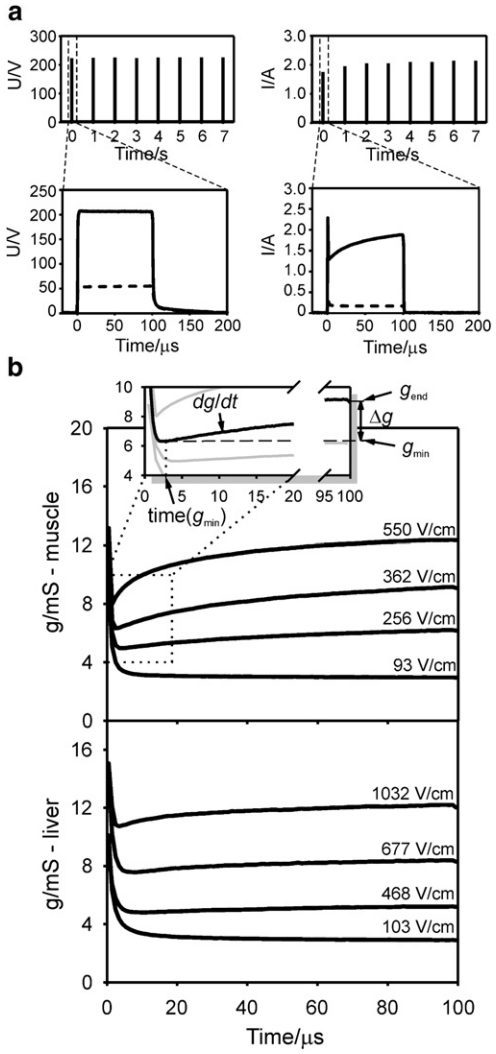

Fig. 2. Electrical properties of tissues during the pulse. (a) Voltage and current traces for below reversible (dashed line) and reversible electroporation settings (solid line). (b) Conductance (g=I/U) of muscle and liver tissue during the pulse. The electric field strength reported is the ratio of the applied voltage to electrodes distance (U/d).

electroporation were determined as the field intensities corresponding to intersections of consecutive linear regressions.

For the demonstration of the efficacy of the proposed algorithm for real time electroporation control (Fig. 4) appropriate software was developed and installed in a Cliniporator™ (IGEA) instrument that was then used to deliver voltage pulses (amplitude 600 V and duration 100 μs) to rabbit skeletal muscle ex-vivo through two plate electrodes. The Cliniporator™ not only delivers pulses but it also measures current and voltage during the pulse with sampling rate 10 MSamples/s as well as it processes measured data in real time. The same instrument was then used in DNA electrotransfer demonstration.

pCMV-Luc+ plasmid containing the cytomegalovirus (CMV) promoter of pcDNA3 (nucleotides 229–890, Invitrogen) inserted upstream of the coding sequence of the firefly luciferase (photinus pyralis) of the pGL2-Basic Vector plasmid (pGL2-Basic Vector, Cat. E1641, Promega) was prepared using the EndoFree Plasmid Giga Kit (QIAGEN). 10 μg of plasmid in 20 μl of PBS were locally injected in the tibial cranial muscle of anesthetized Swiss male mice 10 to 11 weeks old. Using plate electrodes of 5 mm distance, the following transcutaneous electric pulses were delivered using the Cliniporator™: one pulse of 100 μs duration and amplitude 900 V (reduced by algorithm to 460 V) followed by one pulse of 400 ms and 40 V (80 V/cm) [6]. Mice were sacrificed 7 days after DNA injection. Muscles were removed, weighted, and put in one tube of lysing matrix (Bio 101 Systems Lysing Matrix A tube, Qbiogene) containing 1 ml of chilled cell culture lysis reagent solution. This solution was prepared by mixing 10 ml of 5X cell culture lysis reagent (Promega) with 40 ml distilled water supplemented

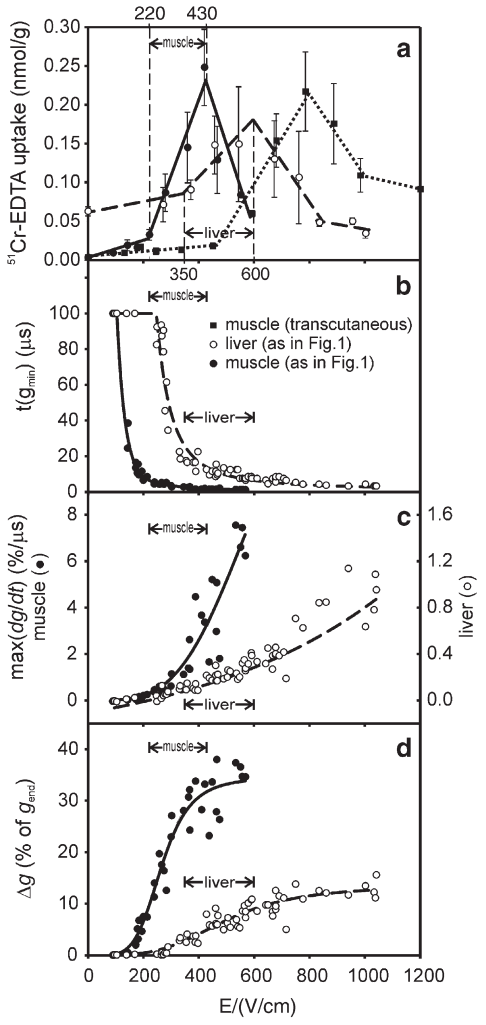

Fig. 3. Reversible and irreversible electric field strength threshold values and parameters for detection of tissue permeabilization. (a) Mean values of ^{51}Cr-EDTA uptake (±SEM) as a function of electric field strength (E) reported as ratio of the applied voltage (U) to electrodes distance (d), in the rat skeletal muscle without the skin (closed circles) and liver (open circles). The ^{51}Cr-EDTA uptake results for the rat skeletal muscle with the skin are presented with closed squares. The reversible electroporation range is graphically displayed in each of the panels, respectively, for the liver and the rat muscle without the skin. Each current sample was divided by the corresponding voltage sample to yield conductance (g=I/U). Parameters for detection of tissue permeabilization are: (b) time elapsed from pulse beginning to minimal conductance as a function of electric field strength, for rat muscle and liver. (c) Conductance maximal slope versus time. (d) Conductance change during the pulse (same symbols).

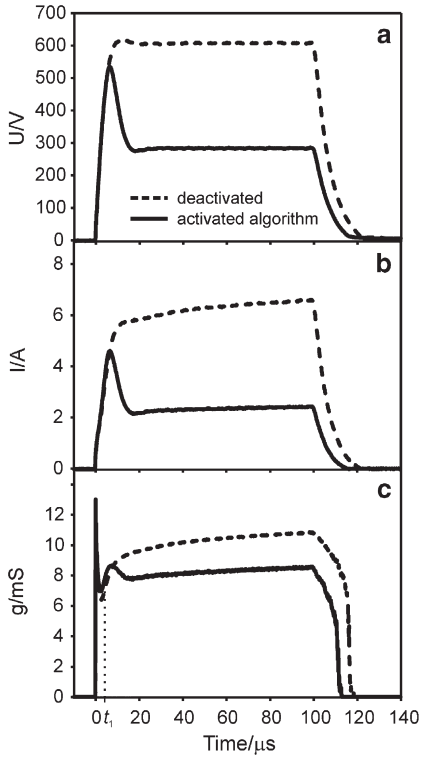

Fig. 4. Demonstration of the algorithm for safe electropermeabilization. Voltage (a), current (b) and conductance (c) traces are presented with solid lines when the algorithm for irreversible electropermeabilization detection was activated and with dashed lines when the algorithm was not active.

with one tablet of protease inhibitor cocktail (Boehringer Mannheim). Muscles were then disrupted using a high-speed benchtop homogenizer (FastPrep® Instrument, Qbiogene). After the lysis the tubes were centrifugated at 12,000 rpm for 10 min. We measured the luciferase activity on 20 μl of the supernatant, using a Lumat LB 9507 luminometer (Berthold France S.A.), by integration of the light produced during 10 s, starting after the addition of 100 μl of Luciferase Assay Substrate (Promega) to the sample lysate. We collected the results from the luminometer in relative light units (RLU). Calibration with purified firefly luciferase protein was used to express the final results as picograms of luciferase per muscle. Serum levels of creatinin kinase (CK), a marker of muscle injury, were measured in 100 μl of blood plasma using a Synchron LX®i 725 Clinical System (Beckman Coulter).

3. Results

Electrical properties of biological tissues are complex and can be modeled by various equivalent electrical circuits composed of capacitors and resistors or by finite elements method to estimate electric field strength distribution in tissue. Fig. 1 displays the experimental settings used on muscle and on liver and the corresponding numerical models. Data shows that in the tissue encompassed by the electrodes, more than 68% of the muscle and more than 81% of the liver was exposed to an electric field strength (± 10%) equivalent to the ratio of the applied voltage to the electrodes distance. It is thus acceptable, in these particular experimental conditions, to consider that electric field strength distribution is sufficiently homogeneous to refer to the electric field strength in the tissue by the value of the ratio of the applied voltage to the electrodes distance.

The electrical current response to a low voltage pulse (no electropermeabilization) applied to the tissue consists of a rapid initial current increase followed by an exponential decrease, as "capacitors" are charging, and a constant level of current after "capacitors" are fully charged, suggesting that the "capacitors" were charged in a few microseconds (Fig. 2a). When the pulse voltage was high enough to permeabilize the tissue, the current was found to further increase during the pulse, as the conductivity of permeabilized tissue increased [18–21] (Fig. 2a). Indeed, unless cells are permeabilized all current passes around the cells, while permeabilization provides additional current paths so the total current increases. Time dynamics of the current increase during the pulse depends on the pulse voltage; however, at our pulse length current always reaches constant level before the pulse ends. In order to analyze these changes independently of pulse voltage, conductance (g), which is the ratio current/voltage, was calculated (Fig. 2b).

Tissue permeabilization was quantified using the 51Cr–EDTA uptake method [12] on the same samples in which current and voltage were recorded, after we demonstrated that 51Cr–EDTA injection did not modify the time course of g (data not shown). Under control conditions (no electric field applied) the average uptake in the liver was 0.073±0.010 nmol/g (mean±std.dev.), while in muscle it was 0.003±0.002 nmol/g, indicating that almost all molecules were washed out from the skeletal muscle in 24 h, while liver tissue was still retaining some 51Cr–EDTA. The 51Cr–EDTA enters the cells and remains entrapped inside the cells only if cells are reversibly permeabilized (if cells are irreversibly permeabilized, the 51Cr–EDTA leaks out of the cells). In rat skeletal muscle directly exposed to the electric pulses, 51Cr–EDTA retention 24 h after the injection significantly increased at field intensities above 220 V/cm (Fig. 3a). Uptake increased with increasing electric field intensity until 430 V/cm. When the field intensity was further increased, uptake was significantly reduced, which reflects the onset of irreversible permeabilization. For transcutaneous pulses, uptake in the skeletal muscle showed the same pattern but at higher field strengths (Fig. 3a). Uptake results in rat liver were much more scattered than in skeletal muscle and statistical analysis in liver did not reveal significant uptake changes. Nevertheless, a clear increase of uptake in liver was found at field intensities above 350 V/cm, with maximum uptake at 600 V/cm and decreasing uptake at higher field intensities.

Time courses of g for rat muscle and liver at various electric field intensities are presented in Fig. 2b. At permeabilizing electric field intensities, it can be seen that, after a very fast rise and a fast decrease (transient which is result of charging of the tissue "capacitors"), g is then increasing during the rest of the pulse delivery, and furthermore increases faster and reaches higher levels at higher electric field intensities. We decided to relate dynamics of g during the pulse to the level of tissue electropermeabilization and to seek for reliable parameters linking dynamics of g to the tissue electropermeabilization level. Detailed mathematical analysis of g time courses was performed and many

parameters of this curves plotted as a function of the applied field strength. The following parameters (Fig. 3b, c and d) showed clear relationship with permeabilization levels and could be used for real time pulse control: (1) the time elapsed from the pulse beginning to the minimal value of g ($t(g_{min})$ in μs) (Fig. 3b), (2) the slope of g versus time normalized to the g value at the time of calculation at $t > t(g_{min})$ (dg/dt in %/μs) (Fig. 3c), (3) the total change in g values, describing the percent difference between g at the end of pulse and the minimal g (Δg in % of g at the end of pulse) (Fig. 3d).

As for the minimum, the following control algorithm can be proposed: (1) if the minimum is detected at time periods shorter than 1.8 μs and 6.2 μs after pulse application to rat skeletal muscle and liver, respectively (Fig. 3b), the electric field intensity is too high and should be lowered in order to assure no irreversible tissue damages related to irreversible membrane permeabilization; (2) if the minimum is detected at time periods longer than 6.2 μs in muscle and 25 μs in liver after the pulse beginning, electric field intensity has to be increased to obtain tissue permeabilization.

If the minimum is found within the expected time interval, the electroporation process can also be monitored later. Indeed, the slope of g versus time calculated in real time after the minimum can be used to verify the tissue electropermeabilization and that the process is reversible. The algorithm should then consider that a slope for rat skeletal muscle between 0.30 and 3.30%/μs assures that tissue will be reversibly permeabilized with eight 100 μs long pulses (Fig. 3c). The slope should fall within a range of 0.08 and 0.28%/μs for liver. If the slope is not in the expected range, pulse delivery should be readjusted. Thus, combinations of controls based on the time of the minimum and on slope measurement can be used for real time pulse adjustment.

Of course, after the first pulse is completely delivered, an *a posteriori* validation could be performed as suggested by Davalos et al. [22]. A g change during the pulse in the range between 9.6% and 31.8% for muscle and in the range between 2.9% and 9.0% for liver assures that tissue was reversibly electropermeabilized (Fig. 3c). Lower values indicate insufficient permeabilization whereas higher values indicate irreversible damages.

Appropriate software can determine and process $t(g_{min})$ and/or dg/dt in μs time range. Moreover, the high voltage generator needs just few μs to readjust the voltage. Thus no technical barrier exists to implement this method for real time detection and control of in vivo electropermeabilization. Our findings were already implemented in a prototype device and demonstrated ex-vivo on muscle tissue (Fig. 4). Using plate electrodes with 0.6 cm distance, pulses of 600 V were delivered. The prototype device was programmed to find minimal conductance, and when found, to calculate the conductance slope. The algorithm was set to decrease the output voltage to a half immediately after conductance slope exceeds 3.3%/ms. In the *ex vivo* experiment the prototype found minimal conductance at 2.4 μs after pulse beginning. With deactivated algorithm the maximal conductance slope was 6.2%/ms. In the experiment presented in Fig. 4, where electrodes were in direct contact with the muscle, the slope exceeded threshold value 3.3%/ms at $t_1 = 3.95$ μs after pulse beginning. After only 0.7 μs the microprocessor corrected the output voltage setting it to 300 V.

Even though the algorithm was determined and tested *ex vivo* in the simplest experimental design (electrodes in direct contact with the tissue, Fig. 1), we further demonstrated its use in vivo in gene transfer experiments, where pulses are usually delivered transcutaneously. The presence of the skin not only introduces more complexity in the theoretical and numerical analysis [23], but it also requires higher pulse amplitudes to achieve permeabilization levels comparable to those achieved with electrodes in direct contact with the muscle (the reversible permeabilization threshold for rat muscle with the skin was 460 V/cm and the irreversible permeabilization threshold was 790 V/cm at 8 times 100 μs pulse parameters, Fig. 3a). DNA coding for the firefly luciferase was injected in the *tibialis cranialis* muscle in mice and, to permeabilize the muscle, one 900 V transcutaneous pulse was applied to the mice leg using external electrodes 5 mm apart. This field strength was applied as being excessive while the reduction in 50% imposed by the algorithm is close to the optimal predicted values according to Fig. 3a. This permeabilizing pulse was followed by one electrophoretic pulse of 400 ms to allow DNA uptake by the electropermeabilized muscle fibres [6]. In a preliminary experiment, the muscles exposed to 900 V pulses without activation of the algorithm (900/900 muscles, $n = 2$) gave a luciferase expression level (1.02 ± 1.44 pg of luciferase/muscle) 200 times lower than the muscles exposed to 900 V pulses with the activated algorithm (900/460 muscles, $n = 3$; 202 ± 134 pg of luciferase/muscle). Data is expressed in pg of luciferase/muscle because the muscles exposed to uncorrected 900 V pulses were damaged and their weight significantly ($p < 0.05$) reduced by 46% (at an average of 64 ± 23 mg per muscle) with respect to the 900/460 muscles (119 ± 17 mg per muscle). In the second experiment ($n = 4$ in both groups) the luciferase expression level in the 900/900 muscles (34 ± 21 pg of luciferase/muscle) was significantly lower (60 times; $p < 0.05$) than in the 900/460 muscles (2064 ± 1181 pg of luciferase/muscle). The reduction of the weight of the 900/900 muscles was less severe than in the preliminary experiment (of 12% only, at 103 ± 11 mg versus 117 ± 14 mg in the 900/460 muscles). In this second experiment, we also measured the serum levels of creatinin kinase (CK, a marker of muscle injury) three days after the electric treatment: the CK levels in the 900/900 mice (183 ± 23 IU/l) were significantly ($p < 0.01$) higher than those of the 900/460 mice (107 ± 30 IU/l). Both the CK levels and muscle weight loss show that the algorithm activation largely protected the muscles from the damages of muscle exposure to excessive field strength. This protection also allows maintaining high levels of expression of the electrotransferred gene.

4. Discussion

In our study we describe and demonstrated a real time detection method of tissue permeabilization. Current and voltage recording during the pulse is easy and can be analyzed in real time. To our knowledge, no other available approach can be used to adjust the pulse voltage in real time in order to ascertain the

achievement of reversible tissue permeabilization. Electrical impedance tomography [22] using a single frequency record requires calculations that can only be completed after the end of the pulse. Tissue impedance changes at various frequencies or even at single frequency in the range up to 100 kHz cannot be acquired in less than 100 μs. Thus they are only interesting for postpulse versus prepulse comparisons, provided of course that no position changes of the electrodes occur during the pulse. At least for muscle electroporation, it is very difficult to avoid such changes due to muscle contraction during pulse delivery.

Analysis of electrical parameters was performed on the first pulse only, while electroporation level was determined based on a train of eight pulses. In fact, current/voltage changes were recorded for the eight pulses using the segmentation function of the oscilloscope and similar variations were observed in the eight pulses of a given train of pulses (data not shown). Thus, to achieve the expected electroporation level it is sufficient to measure the parameters of the first pulse, to adjust them in real time as proposed above and then to administer seven additional pulses [21]. Alternatively the high voltage pulse can be followed by low voltage electrophoretic pulses for DNA transfection [6]. One of the advantages of being able to check electropermeabilization level after one pulse instead of after a full sequence is that it could minimize discomfort to a patient.

The electric field strength threshold values for reversible and irreversible permeabilization are in agreement with previously reported knowledge. In a previous study [13], we used needle electrodes in rabbit liver and calculated the electric field strength distribution in the tissue by numerical modeling. Based on biological observations of drug delivery in in vivo experiments we determined the reversible (362±21 V/cm) and irreversible (637±43 V/cm) electric field strength threshold values for rabbit liver. These values are almost identical to our present measurements in rat liver. Threshold values are considerably lower in rat muscle than in rat liver (Fig. 3a). This can be explained by the fact that the liver cells, smaller, must be exposed to a higher electric field intensity than the skeletal muscle cells, larger, to induce the same transmembrane voltage in agreement with Schwan's equation [24] as well as with more recent determinations of the transmembrane potential changes on spheroidal cells [25,26]. Previous threshold determinations in skeletal muscle were performed in mice, using transcutaneous pulses [11,12]. In fact our parallel determinations in rats using transcutaneous pulses (data not shown) demonstrate that thresholds in skeletal muscle with skin are almost identical in rats (550 V/cm) and in mice (530 V/cm). We can conclude that differences between tissues are much larger than differences between species, at least among the common laboratory animals. Thus it can be speculated that the algorithm, with minor adaptations, could also operate in larger animals and even in humans.

In summary, as we demonstrated, it is possible to achieve electric pulses safe delivery by real time voltage control. Safer (controlled) electropermeabilizing pulses actually resulted in the protection of the tissue in gene transfer experiments where excessive applied voltages lead to intense muscle damage and loss of the efficacy of the gene transfer. Thus safe gene electrotransfer can be achieved without the need of previous precise tuning of the experimental conditions, a situation that can be very useful in the clinical settings.

Electrogenetherapy is one of the most efficient non-viral approaches for gene therapy [3–5]. It was already considered a safe method because naked DNA is not immunogenic (unlike adenoviruses in particular) and plasmid DNA does not need to contain insertion promoting sequences (like the retroviral and lentiviral vectors) which can result in deleterious insertional mutagenesis [27]. Moreover, DNA electrotransfer can be accomplished using devices that are already used on human cancer patients to deliver cytotoxic molecules like bleomycin and cisplatin to solid tumors by electrochemotherapy [28–31]. Thus all elements are available for safe and widespread use of this efficient technology and for implementing the use of genes for biomedical purposes in the post human genomic era [32].

Acknowledgements

This research was supported by the CNRS, the Institut Gustave–Roussy and the Cliniporator project (FP5, Contract No. QLK3–1999–00484) of the European Community. We also acknowledge the staff of the Service Commun d'Expérimentation Animale (M. P. Ardouin) of the Institut Gustave–Roussy for animal maintenance, and France Télécom (Dr. J. Wiart) for the generous loan of the oscilloscope and the recording material (probes, portable computer and software). The authors are in debt to Selma Čorović (Faculty of Electrical Engineering, University of Ljubljana, Slovenia) for her finite element modeling of electric field strength distribution in tissues and to Claudio Bertacchini (IGEA s.r.l., Carpi, Italy) for testing the algorithm ex-vivo on tissue.

References

[1] L.M. Mir, Therapeutic perspectives of in vivo cell electropermeabilization, Bioelectrochemistry 53 (2001) 1–10.
[2] M.P. Rols, C. Delteil, M. Golzio, P. Dumond, S. Cros, J. Teissie, In vivo electrically mediated protein and gene transfer in murine melanoma, Nat. Biotechnol. 16 (1998) 168–171.
[3] L.M. Mir, M.F. Bureau, J. Gehl, R. Rangara, D. Rouy, J.M. Caillaud, P. Delaere, D. Branellec, B. Schwartz, D. Scherman, High-efficiency gene transfer into skeletal muscle mediated by electric pulses, Proc. Natl. Acad. Sci. U. S. A. 96 (1999) 4262–4267.
[4] C. Bloquel, E. Fabre, M.F. Bureau, D. Scherman, Plasmid DNA electrotransfer for intracellular and secreted proteins expression: new methodological developments and applications, J. Gene Med. 6 (2004) S11–S23.
[5] F. André, L.M. Mir, DNA electrotransfer: its principles and an updated review of its therapeutic applications, Gene Ther. 11 (2004) S33–S42.
[6] S. Satkauskas, M.F. Bureau, M. Puc, A. Mahfoudi, D. Scherman, D. Miklavčič, L.M. Mir, Mechanisms of in vivo DNA electrotransfer: respective contributions of cell electropermeabilization and DNA electrophoresis, Molec. Ther. 5 (2002) 133–140.
[7] J. Teissie, T.Y. Tsong, Electric-field induced transient pores in phospholipid-bilayer vesicles, Biochemistry 20 (1981) 1548–1554.
[8] S. Orlowski, L.M. Mir, Cell electropermeabilization — a new tool for biochemical and pharmacological studies, Biochim. Biophys. Acta 1154 (1993) 51–63.
[9] E. Neumann, S. Kakorin, K. Toensing, Membrane electroporation and electromechanical deformation of vesicles and cells, Faraday Discuss. 111 (1998) 111–125.

[10] S. Somiari, J. Glasspool-Malone, J.J. Drabick, R.A. Gilbert, R. Heller, M.J. Jaroszeski, R.W. Malone, Theory and in vivo application of electroporative gene delivery, Molec. Ther. 2 (2000) 178–187.
[11] J. Gehl, L.M. Mir, Determination of optimal parameters for in vivo gene transfer by electroporation, using a rapid in vivo test for cell permeabilization, Biochem. Biophys. Res. Commun. 261 (1999) 377–380.
[12] J. Gehl, T.H. Sorensen, K. Nielsen, P. Raskmark, S.L. Nielsen, T. Skovsgaard, L.M. Mir, In vivo electroporation of skeletal muscle: threshold, efficacy and relation to electric field distribution, Biochim. Biophys. Acta 1428 (1999) 233–240.
[13] D. Miklavčič, D. Šemrov, H. Mekid, L.M. Mir, A validated model of in vivo electric field distribution in tissues for electrochemotherapy and for DNA electrotransfer for gene therapy, Biochim. Biophys. Acta 1523 (2000) 73–83.
[14] D. Šel, D. Cukjati, D. Batiuskaite, T. Slivnik, L.M. Mir, D. Miklavčič, Sequential Finite Element Model of Tissue Electropermeabilization, IEEE Trans. Biomed. Eng. 52 (2004) 816–827.
[15] E. Neumann, S. Kakorin, K. Toensing, Fundamentals of electroporative delivery of drugs and genes, Bioelectrochem. Bioenerg. 48 (1999) 3–16.
[16] P. Workman, P. Twentyman, F. Balkwill, A. Balmain, D. Chaplin, J. Double, J. Embleton, D. Newell, R. Raymond, J. Stables, T. Stephens, J. Wallace, United Kingdom Co-Ordinating Committee on Cancer Research (UKCCCR) Guidelines for the Welfare of Animals in Experimental Neoplasia, Second Edition, Br. J. Cancer, vol. 77, 1998, pp. 1–10.
[17] B. Irons, S. Ahmad, Techniques of finite elements, John Wiley & Sons, New York, 1986.
[18] M. Hibino, M. Shigemori, H. Itoh, K. Nagayama, K. Kinosita, Membrane conductance of an electroporated cell analyzed by submicrosecond imaging of transmembrane potential, Biophys. J. 59 (1991) 209–220.
[19] I.G. Abidor, A.I. Barbul, D.V. Zhelev, P. Doinov, I.N. Bandrina, E.M. Osipova, S.I. Sukharev, Electrical properties of cell pellets and cell electrofusion in a centrifuge, Biochim. Biophys. Acta 1152 (1993) 207–218.
[20] M. Pavlin, D. Miklavčič, Effective conductivity of a suspension of permeabilized cells: a theoretical analysis, Biophys. J. 85 (2003) 719–729.
[21] M. Pavlin, M. Kandušer, M. Reberšek, G. Pucihar, F.X. Hart, R. Magjarević, D. Miklavčič, Effect of cell electroporation on the conductivity of a cell suspension, Biophys. J. 88 (2005) 4378–4390.
[22] R.V. Davalos, B. Rubinsky, D.M. Otten, A feasibility study for electrical impedance tomography as a means to monitor tissue electroporation for molecular medicine, IEEE Trans. Biomed. Eng. 49 (2002) 400–403.
[23] N. Pavšelj, Z. Bregar, D. Cukjati, D. Batiuskaite, L.M. Mir, D. Miklavčič, The course of tissue permeabilization studied on a mathematical model of a subcutaneous tumor in small animals, IEEE Trans. Biomed. Eng. 52 (2005) 1373–1381.
[24] H. Pauly, H.P. Schwan, Über die Impedanz einer Suspension von kugelförmigen Teilchen mit einer Schale, Z. Naturforsch. 14B (1959) 125–131.
[25] B. Valič, M. Golzio, M. Pavlin, A. Schatz, C. Faurie, B. Gabriel, J. Teissie, M.P. Rols, D. Miklavčič, Effect of electric field induced transmembrane potential on spheroidal cells: theory and experiment, Eur. Biophys. J. 32 (2003) 519–528.
[26] T. Kotnik, D. Miklavčič, Analytical description of transmembrane voltage induced by electric fields on spheroidal cells, Biophys. J. 79 (2000) 670–679.
[27] Z.X. Li, J. Dullmann, B. Schiedlmeier, M. Schmidt, C. von Kalle, J. Meyer, M. Forster, C. Stocking, A. Wahlers, O. Frank, W. Ostertag, K. Kuhlcke, H.G. Eckert, B. Fehse, C. Baum, Murine leukemia induced by retroviral gene marking, Science 296 (2002) 497.
[28] M. Belehradek, C. Domenge, B. Luboinski, S. Orlowski, J. Belehradek, L.M. Mir, Electrochemotherapy, a new antitumor treatment — 1st clinical phase-I-II trial, Cancer 72 (1993) 3694–3700.
[29] L.M. Mir, L.F. Glass, G. Serša, J. Teissie, C. Domenge, D. Miklavčič, M.J. Jaroszeski, S. Orlowski, D.S. Reintgen, Z. Rudolf, M. Belehradek, R. Gilbert, M.P. Rols, J. Belehradek, J.M. Bachaud, R. DeConti, B. Stabuc, M. Čemažar, P. Coninx, R. Heller, Effective treatment of cutaneous and subcutaneous malignant tumours by electrochemotherapy, Br. J. Cancer 77 (1998) 2336–2342.
[30] A. Gothelf, L.M. Mir, J. Gehl, Electrochemotherapy: results of cancer treatment using enhanced delivery of bleomycin by electroporation, Cancer Treat. Rev. 29 (2003) 371–387.
[31] G. Serša, M. Čemažar, Z. Rudolf, Electrochemotherapy: advantages and drawbacks in treatment of cancer patients, Cancer Ther. 1 (2003) 133–142.
[32] D. Ferber, Gene therapy: safer and virus-free? Science 294 (2001) 1638–1642.